

SImpHAR: Advancing impedance-based human activity recognition using 3D simulation and text-to-motion models

Lala Shakti Swarup Ray
DFKI, RPTU
Kaiserslautern, Germany
lala_shakti_swarup.ray@dfki.de

Mengxi Liu
DFKI, RPTU
Kaiserslautern, Germany
mengxi.liu@dfki.de

Deepika Gurung
DFKI, RPTU
Kaiserslautern, Germany
deepika.gurung@dfki.de

Bo Zhou
DFKI, RPTU
Kaiserslautern, Germany
bo.zhou@dfki.de

Sungho Suh*
Korea University
Seoul, Republic of Korea
Sungho_Suh@Korea.ac.kr

Paul Lukowicz
DFKI, RPTU
Kaiserslautern, Germany
paul.lukowicz@dfki.de

Abstract

Human Activity Recognition (HAR) with wearable sensors is essential for applications in healthcare, fitness, and human-computer interaction. Bio-impedance sensing offers unique advantages for fine-grained motion capture but remains underutilized due to the scarcity of labeled data. We introduce SImpHAR, a novel framework addressing this limitation through two core contributions. First, we propose a simulation pipeline that generates realistic bio-impedance signals from 3D human meshes using shortest-path estimation, soft-body physics, and text-to-motion generation serving as a digital twin for data augmentation. Second, we design a two-stage training strategy with decoupled approach that enables broader activity coverage without requiring label-aligned synthetic data. We evaluate SImpHAR on our collected ImpAct dataset and two public benchmarks, showing consistent improvements over state-of-the-art methods, with gains of up to 22.3% and 21.8%, in terms of accuracy and macro F1 score, respectively. Our results highlight the promise of simulation-driven augmentation and modular training for impedance-based HAR.

CCS Concepts

• **Computing methodologies** → **Learning paradigms**; *Shape analysis*; **Learning paradigms**.

Keywords

HAR, bio-impedance, simulation, sensor, wearable computing

ACM Reference Format:

Lala Shakti Swarup Ray, Mengxi Liu, Deepika Gurung, Bo Zhou, Sungho Suh, and Paul Lukowicz. 2018. SImpHAR: Advancing impedance-based human activity recognition using 3D simulation and text-to-motion models. In *Proceedings of Make sure to enter the correct conference title from your*

*Corresponding Author

Permission to make digital or hard copies of all or part of this work for personal or classroom use is granted without fee provided that copies are not made or distributed for profit or commercial advantage and that copies bear this notice and the full citation on the first page. Copyrights for components of this work owned by others than the author(s) must be honored. Abstracting with credit is permitted. To copy otherwise, or republish, to post on servers or to redistribute to lists, requires prior specific permission and/or a fee. Request permissions from permissions@acm.org.

Conference acronym 'XX, Woodstock, NY

© 2018 Copyright held by the owner/author(s). Publication rights licensed to ACM.
ACM ISBN 978-1-4503-XXXX-X/2018/06
<https://doi.org/XXXXXXXX.XXXXXXX>

rights confirmation email (Conference acronym 'XX). ACM, New York, NY, USA, 8 pages. <https://doi.org/XXXXXXXX.XXXXXXX>

1 Introduction

Human Activity Recognition (HAR) using wearable sensors is foundational in healthcare, fitness, industrial safety, and human-computer interaction [2, 4, 13, 31, 42, 48]. The performance of HAR systems heavily depends on the sensing modality. While prior work has explored inertial, acoustic, field-based, and physiological sensors [1, 6], bio-impedance remains significantly underexplored—despite its ability to capture fine-grained physiological changes that many modalities overlook.

Bio-impedance measures the opposition of biological tissue to a small electrical current passed between electrodes on the body. This impedance changes with posture, motion, muscle activation, and tissue deformation—making it potentially powerful for capturing subtle motion dynamics. Its applications extend from body composition analysis [24], respiration [17], and heart rate [10, 38], to dynamic contexts like gesture recognition [3, 20], dietary monitoring [22], and activity tracking [21, 37]. Despite these promising properties, bio-impedance-based HAR suffers from two major limitations: (1) the scarcity of large-scale, labeled datasets due to hardware complexity and the need for careful electrode placement; and (2) intra-user variability caused by physiological factors such as hydration level, muscle mass, and skin contact quality. These challenges hinder reproducibility and limit generalization across users. Meanwhile, mature sensing modalities like IMUs benefit from public benchmarks [5, 40, 46] and established data augmentation pipelines [8, 14, 18, 51]. To bridge the gap, simulation-based frameworks have emerged in HAR research—using digital twins to generate synthetic sensor signals from video, pose, or text [33, 35, 36, 47]. However, none of these approaches address bio-impedance, primarily because: (1) it has been historically treated as noise in motion contexts, and (2) no well-established model exists to map motion dynamics to time-varying impedance.

To address these gaps, we introduce **SImpHAR**, the first framework for simulating user-specific bio-impedance signals from 3D motion and textual descriptions. It consists of two components: (1) Pose2Imp that simulates impedance dynamics from 3D body mesh sequences using shortest-path estimation, soft-body physics, and neural signal transformation. (2) Text2Imp that uses generative motion models to convert textual activity descriptions into

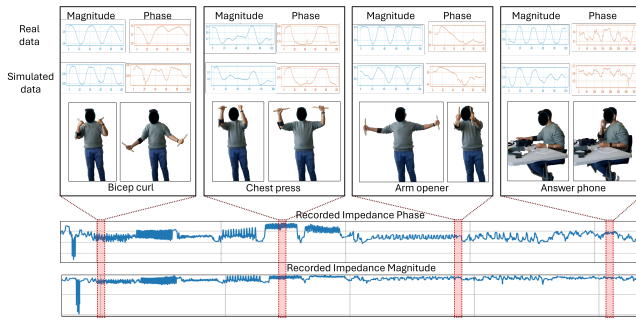


Figure 1: Synthesized impedance signal (SImp) vs. real impedance signal (IMP) magnitude generated using SImpHAR.

pose sequences, then synthesizes corresponding impedance signals via Pose2Imp. Unlike prior approaches that naively mix synthetic and real data, we propose **SImpHARNet**, a two-stage learning strategy designed to preserve domain alignment: (1) Contrastive Pretraining: Aligns simulated impedance and text embeddings to build semantically meaningful shared representations, and (2) Fine-tuning: Adapts the model to a target task using limited real-world impedance data. We further introduce **ImpAct**, a new multimodal dataset of synchronized impedance, video, and 3D pose recordings across ten everyday activities and ten participants. This dataset fills a crucial gap for benchmarking impedance-based HAR models.

Our key contributions are:

- **SImpHAR**, a simulation framework that generates realistic bio-impedance signals from motion and text, enabling scalable and controllable data synthesis.
- **SImpHARNet**, a decoupled training pipeline combining contrastive pretraining and fine-tuning for effective domain adaptation to real-world tasks.
- **ImpAct**, a new dataset for impedance-based HAR, offering aligned video, 3D pose, activity annotations, and wearable sensor data (Figure 1).

2 Related Work

A primary challenge in impedance-based HAR is the lack of large, labeled datasets. As with other sensor modalities, collecting synchronized and annotated data is expensive and labor-intensive. Prior efforts have addressed this gap through sensor simulation and cross-modal representation learning.

Sensor Simulation: Several simulation frameworks generate synthetic sensor data using video, motion capture, or text. IMUTube [14] and Cromosim [12] synthesize inertial signals from pose data, while PresSim [35] and PressureTransferNet [33] produce pressure maps from video. Capafoldable [30, 32] applies a similar approach to simulate capacitive signals for smart textiles. Recent methods extend this idea by coupling text-to-motion generation with simulators, enabling sensor synthesis from natural language prompts. IMUGPT [18] and T2P [34] generate inertial or pressure data using IMUSim [47] and PresSim. While effective, these pipelines often struggle with domain-specific activity coverage due to the limited motion diversity of generative models. Moreover, mixing synthetic

and real data without alignment can lead to performance degradation. Our method addresses this by decoupling representation learning from task fine-tuning: SImpHARNet uses contrastive pre-training on large-scale simulated data followed by adaptation on small, labeled real-world samples.

Representation Learning: Contrastive and self-supervised learning have shown strong results in HAR by aligning representations across heterogeneous modalities [7, 9, 43]. IMU2CLIP [25] projects IMU signals into shared embeddings with images and text via CLIP [29]. iMove [21] jointly embeds IMU and impedance signals, while others [15, 16, 27] demonstrate the benefits of training with richer sensor or auxiliary modalities. Building on these insights, we simulate impedance signals at scale using motion and text inputs, then use contrastive learning to align them with corresponding descriptions. This enables SImpHARNet to generalize across activity classes—even when synthetic and real-world categories are not perfectly aligned—making it effective in data-scarce regimes.

3 Approach

The proposed approach, SImpHAR, addresses the data scarcity and modeling challenges in impedance-based HAR by introducing a simulation-to-training pipeline that can generate realistic, personalized impedance signals from motion data and support robust downstream learning. At the core is a simulation framework called Pose2Imp, which models impedance dynamics from 3D human pose using shortest-path analysis, soft-body deformation, and a neural grounding module that personalizes the signals based on physiological traits. Text2Imp complements this by leveraging generative text-to-motion models to produce diverse activity sequences from textual prompts, which are then converted into impedance signals via Pose2Imp. To overcome the limitations of Text-to-motion generative models in generating domain specific actions, we introduce SImpHARNet, a two-stage learning strategy that first performs contrastive pretraining on large-scale simulated impedance-text pairs to learn generalizable embeddings, and then fine-tunes the model on a small set of real, labeled signals. This decoupled design allows the model to benefit from diverse, unlabeled motion data during pretraining while ensuring adaptation to the target domain during fine-tuning.

3.1 Pose2Imp

Our method is based on the observation that bio-impedance is influenced by the path of least resistance (i.e., the shortest conductive path) between two electrodes on the body. As the body moves, this path dynamically changes—making it a proxy for estimating time-varying impedance signals.

Shortest Path Estimation. We use OSX [19] to estimate SMPL-H [23] meshes from video. The body mesh is modeled as a graph where vertices represent surface points and edge weights correspond to Euclidean distances.

We adapt Dijkstra’s algorithm [50] to compute frame-wise shortest paths between electrode positions on the 3D body mesh. Unlike the standard algorithm that minimizes hop count, we assign edge weights using Euclidean distances between mesh vertices—yielding geodesic paths that approximate conductive paths relevant to bio-impedance.

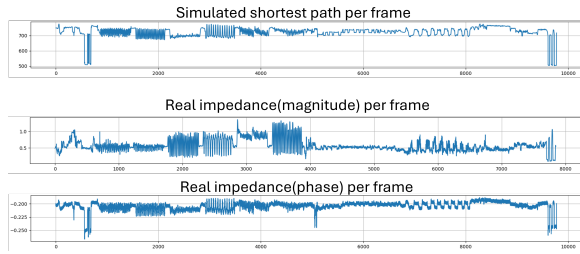


Figure 2: Direct correlation between impedance magnitude, phase, and simulated shortest path.

Algorithm 1 Dijkstra’s Algorithm with Euclidean Weights on Mesh

```

1:  $d[v] \leftarrow \infty$  for all vertices  $v$ , except source  $s$ :  $d[s] \leftarrow 0$ 
2: Initialize priority queue  $Q$  with  $s$ 
3: while  $Q$  not empty do
4:   Extract  $u$  with minimum  $d[u]$ 
5:   for each neighbor  $v$  of  $u$  do
6:      $d[v] \leftarrow \min(d[v], d[u] + \text{dist}(u, v))$ 
7:     if  $d[v]$  updated then
8:       Update  $v$  in  $Q$ 
9:     end if
10:  end for
11: end while

```

This process yields a time-series of shortest path lengths between electrodes, which serve as a geometric approximation of the underlying impedance signal.

Soft Body Simulation. While shortest paths offer a useful structural estimate, they can be biased by mesh discretization and surface topology. To improve realism, we embed a deformable soft-body along the computed path, treating the SMPL mesh as a rigid scaffold. The soft body is initialized with the shortest-path vertices and then deformed using internal strain dynamics to produce a smoothed, continuous path. This step decouples the path shape from mesh resolution and results in more physiologically plausible impedance variation, as shown in Figure 2.

User-Specific Grounding via Neural Mapping. Simulated paths alone do not capture individual physiological factors such as body composition, hydration level, or muscle-to-fat ratio—all of which significantly influence real impedance measurements. To bridge this gap, we introduce a neural mapping module that calibrates the simulated signal to user-specific impedance dynamics.

We adopt a dual-encoder architecture inspired by PresSim [35], illustrated in Figure 3. The network takes as input both the geometric simulation and the user’s pose, and outputs a calibrated impedance signal:

- **SimpPath Encoder:** A bidirectional LSTM that encodes the sequence of simulated path lengths with shape $(\text{window}, 1)$, where window refers to a temporal segment of 60 frames (2 seconds).
- **Pose Encoder:** A parallel bidirectional LSTM that processes SMPL pose parameters with shape $(\text{window}, 52, 3)$ corresponding to 52 joints and 3 rotation axes.

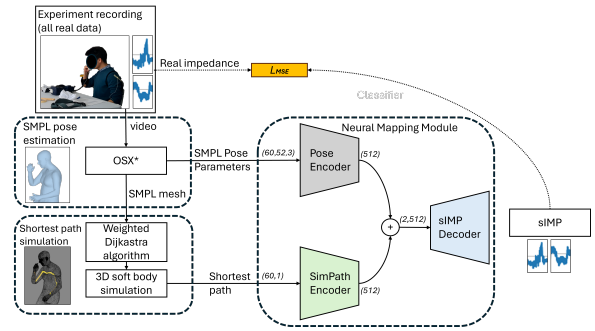


Figure 3: Pose2Imp simulation involves shortest path estimation, followed by soft body simulation and user-specific grounding through neural mapping.

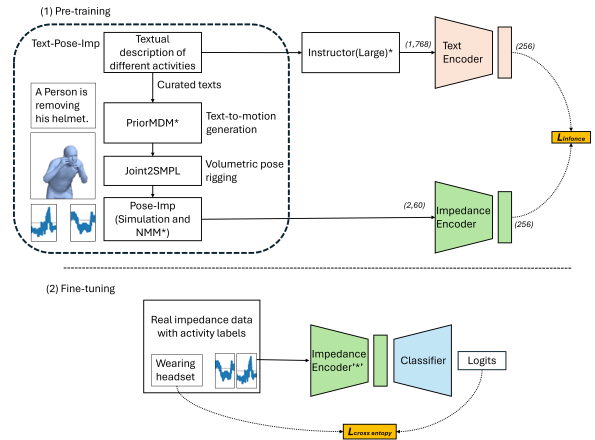


Figure 4: SimpHARNet consists of 2 steps (1) pretraining with simulated data and text embedding for joint representation and (2) downstream classifier training using the pretrained Impedance encoder for HAR (depicts pretrained models).**

- **CNN Decoder:** A convolutional decoder that fuses the two 512-dimensional encoder outputs and predicts the impedance magnitude and phase as a vector of shape $(1, 2)$.

The model is trained using paired real-world impedance and pose data with a Mean Squared Error (MSE) loss. This supervised grounding step enables the framework to personalize the simulated signals—ensuring that the output better reflects actual sensor behavior for a given individual.

3.2 Text2Imp

Manually collecting and labeling real-world videos that resemble target activities is slow, labor-intensive, and often requires physical supervision. As an alternative, text-to-motion generative models offer a scalable way to produce 3D motion data from textual descriptions. However, these models are inherently limited by the motion diversity of their training datasets. For example, common datasets like HumanML3D [11] and KIT-ML [28] do not include

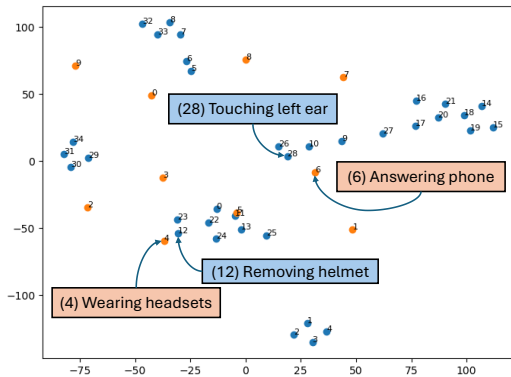


Figure 5: Text embeddings of target classes (orange) and pre-training classes used for generating SImp signals (blue).

actions such as "wearing VR glasses," making it impossible for the models to generate such motions directly.

To address this limitation, we leverage the generative flexibility of PriorMDM [39], a diffusion-based text-to-motion model, to synthesize motions that are semantically similar to our target activities. For each class in our dataset, we craft three related textual descriptions that reflect a similar motion range (e.g., "removing a helmet", "touching both ears" etc as a proxy for "wearing a VR headset") and generate at least ten variations per description, resulting in 30 motion samples per class.

The generated 3D pose sequences are converted into SMPL meshes using joint2SMPL and passed through our Pose2Imp simulation pipeline to produce synthetic impedance signals (SImp). While the generated motions do not exactly replicate those in our real dataset, they capture structurally similar dynamics. As shown in Figure 5, t-SNE visualization [44] of activity text embeddings illustrates strong alignment between real and synthetic samples, validating the semantic consistency of our approach.

3.3 SImpHARNet

To address the limitations of generative models—which often fail to produce domain-specific activities (e.g., wearing a VR headset)—and to avoid performance degradation from naively mixing real and synthetic data, we adopt a two-stage training strategy. As visualized in Figure 4, we first pretrain using bi-modal contrastive learning on synthetic impedance-text pairs, followed by fine-tuning on a small set of labeled real-world data.

Pretraining. The first stage trains our contrastive representation learning model, **SImpHARNet**, to align synthetic impedance signals (SImp) with their associated textual prompts. The goal is to create a shared embedding space where semantically related pairs are close together, enabling generalization to unseen or low-resource activity classes.

SImpHARNet consists of two parallel encoders:

- A fully connected (FC) text encoder with three linear layers, batch normalization, dropout, and GeLU activations.

- A DeepConvLSTM-inspired impedance encoder that transforms a 60-frame SImp window into a 256-dimensional feature vector.

Text prompts are first encoded using Instructor (Large) [41], a pre-trained language model that produces a 1,768-dimensional sentence embedding. Each contrastive training pair consists of a text prompt and its corresponding synthetic impedance signal.

Matched pairs are generated by feeding a specific prompt (e.g., "removing a helmet") into our Text2Imp pipeline and pairing the resulting SImp signal with the original prompt. Unmatched pairs are sampled by randomly selecting text prompts that describe semantically different activities (e.g., pairing "removing a helmet" with SImp from "answering a phone").

We train the encoders using the InfoNCE loss, which minimizes the distance between matched (positive) pairs while maximizing separation from unmatched (negative) ones:

$$\mathcal{L}_{\text{InfoNCE}}(q, k) = -\frac{1}{N} \sum_{i=1}^N \log \left(\frac{e^{s(q_i, k_i)}}{e^{s(q_i, k_i)} + \sum_{j \neq i} e^{s(q_i, k_j)}} \right) \quad (1)$$

where similarity is computed using cosine distance:

$$s(q, k) = \frac{q \cdot k}{\|q\| \cdot \|k\|} \quad (2)$$

To support semantic alignment, we manually craft three text prompts per target activity class (e.g., "removing helmet", "touching both ears", "putting on a hat" for the action "wearing VR headset"), and use PriorMDM to generate multiple pose sequences per prompt. These are then converted into impedance signals via the Pose2Imp simulation pipeline.

We validate the resulting semantic clusters via t-SNE [44], showing that related real and synthetic activity classes form tight clusters in the embedding space (Figure 5).

Downstream Training. In the second stage, we fine-tune the impedance encoder for the target HAR task using real-world labeled data. A lightweight classification head—consisting of a 1D CNN followed by two fully connected layers—is trained on top of the frozen impedance encoder.

To avoid catastrophic forgetting, the impedance encoder is initially frozen during the first N epochs. Once the classification loss plateaus, we unfreeze the encoder and continue fine-tuning the full model end-to-end. This staged optimization ensures that pretrained semantic representations are preserved while allowing adaptation to the target domain.

4 Experimental Results

4.1 Datasets

ImpAct Dataset. Ten participants (four women and six men), aged 24 to 35 years, with body weights ranging from 50.6 to 88.15 kg and heights between 160 and 188 cm, participated in the study. Each participant performed a total of eight activities: six upper-body fitness exercises and three daily tasks involving fine hand movements. Each session lasted approximately 15 minutes per participant. Participants wore a custom-designed bioimpedance sensing device comprising four components: an analog front-end (AFE), a control module, surface electrodes, and a power supply following the

architecture in Liu et al. [21]. The AFE used the AD5941 chip (Analog Devices) to generate sine-wave voltage stimuli across 0.015 Hz to 200 kHz and capture the resulting current with a high-speed transimpedance amplifier. The control module, based on Nordic’s nRF52840 SoC, communicated with the AFE via SPI and wirelessly streamed the measurements over Bluetooth. Bioimpedance electrodes were placed on both wrists one acting as the transmitter and the other as the receiver forming a closed electrical loop with a shared ground. This configuration allowed impedance to be measured across the upper body in a wearable, non-intrusive setup. Additionally, an IMU was mounted on the dominant wrist for motion tracking. The six fitness exercises included *Box*, *Biceps curl*, *Chest press*, *Shoulder and chest press*, *Arm hold and shoulder press*, and *Arm opener*. The three daily tasks were *Sweeping a table*, *Ring-ing a headphone*, and *Transferring a telephone*, focusing on hand and arm manipulation. Bioimpedance and IMU data were streamed in real time to a JavaScript-based laptop application that supported live visualization and automatic text-based logging. A rear-facing video camera recorded all sessions for manual annotation. After temporal synchronization, all data streams were sampled at 20 Hz and segmented using a sliding window of 50 samples with a step size of 10. A photo of the experimental setup, showing electrode placement and device configuration.

iMove Dataset. The iMove dataset contains synchronized multi-modal sensor data collected from ten participants (four female, six male), aged 24 to 35 years. Each participant performed six upper-body fitness exercises—*Box*, *Biceps Curl*, *Chest Press*, *Shoulder and Chest Press*, *Arm Hold*, and *Arm Opener*—across five consecutive days. The dataset includes bio-impedance signals from both wrists and IMU data from the left wrist. All signals were sampled at 20 Hz and segmented using a sliding window of 50 samples with a step size of 10.

iEat Dataset. The iEat dataset comprises synchronized multi-modal data collected from ten participants, each completing 40 meal sessions in naturalistic dining settings. Participants engaged in a diverse set of dietary-related activities, including *eating with utensils*, *drinking*, *using napkins*, *talking*, and *reaching for condiments*, among others. The dataset captures bio-impedance signals from both wrists using a wearable device, sampled at 20 Hz.

4.2 Training Details

The model is written in PyTorch and trained on a linux device with CUDA support, while the simulation is written in Python using the Blender API. We used 300 epochs and employed early stopping with 15 epochs, ADAMW optimization, and a learning rate of 0.001, the ReduceLR On Plateau, with patience 10. We used a leave-one-user-out cross-validation paradigm to evaluate our model on all three datasets. During training, the training and validation data are split with a 9:1 ratio based on a random split.

4.3 Results

We trained all models five times and report the mean R^2 for SImpHAR’s neural mapping given in Table 2 and macro F1/accuracy for downstream HAR tasks using SImpHARNet given in Table 1.

Table 1: Activity classification results for baseline, TinyHAR [49], M2L [45], SR [21], TCNNet [26] and SImpHARNet (ours) using different strategies. For the iMove and iEat datasets, the given accuracy using M2L, SR, TCNNet, and TinyHAR is reported in the respective dataset papers [21, 22].

Dataset	Model	Accuracy	Macro F1
ImpAct	Baseline classifier (real data)	0.621±0.011	0.595±0.007
	Baseline classifier (real+SImp data)	0.618±0.016	0.581±0.012
	TinyHAR (real+SImp data)	0.633±0.015	0.608±0.011
	M2L (real+SImp data)	0.655±0.014	0.618±0.012
	SR (real+SImp data)	0.661±0.013	0.633±0.011
	TCNNet (real+SImp data)	0.675±0.012	0.648±0.011
	SImpHARNet (frozen) SImpHARNet (fine-tuned)	0.651±0.015 0.775±0.010	0.612±0.009 0.767±0.012
iMove	Baseline classifier (real data)	0.641±0.012	0.636±0.008
	Baseline classifier (real+SImp data)	0.743±0.014	0.739±0.010
	TinyHAR (real+SImp data)	0.755±0.013	0.748±0.012
	M2L (real+SImp data)	0.762±0.012	0.754±0.011
	SR (real+SImp data)	0.770±0.013	0.764±0.012
	TCNNet (real+SImp data)	0.778±0.012	0.771±0.010
	SImpHARNet (frozen) SImpHARNet (fine-tuned)	0.704±0.017 0.763±0.016	0.696±0.011 0.752±0.015
iEat	Baseline classifier (real data)	0.731±0.012	0.718±0.020
	Baseline classifier (real+SImp data)	0.669±0.015	0.651±0.013
	TinyHAR (real+SImp data)	0.650±0.014	0.643±0.012
	M2L (real+SImp data)	0.665±0.013	0.658±0.011
	SR (real+SImp data)	0.680±0.014	0.673±0.012
	TCNNet (real+SImp data)	0.690±0.013	0.683±0.011
	SImpHARNet (frozen) SImpHARNet (fine-tuned)	0.791±0.008 0.844±0.014	0.786±0.012 0.832±0.009

Table 2: Performance of STN trained on different inputs.

TSN Input	R^2
3D Pose	0.414±0.018
Simulated Distance	0.821±0.013
3D Pose + Simulated Distance	0.843±0.025

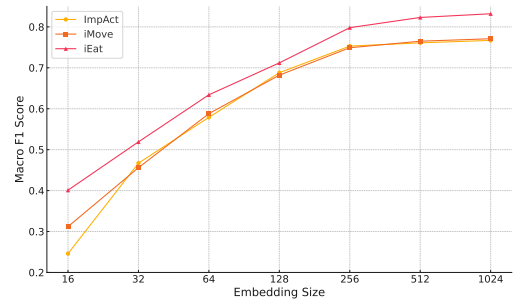


Figure 6: SImpHARNet trained with varying embedding size showcasing the change in F1 based on dimension size.

Effectiveness of Simulated Shortest Path: To evaluate the benefit of our geometric simulation, we trained the STN using only SMPL pose parameters, which yielded an R^2 of 0.414. Incorporating simulated shortest path distances improved performance by nearly 50%, and

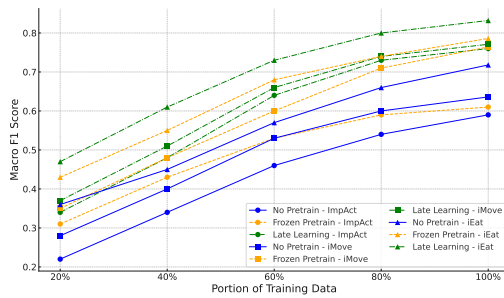


Figure 7: Change in F1 score for classification models trained with different portions of the training set.

combining both inputs yielded the best result ($R^2 = 0.843$), validating the contribution of the path-based simulation.

Impact of Simulated Impedance Data on HAR: We evaluated the effect of augmenting real data with synthetic impedance (SImp) signals for HAR. Across datasets, adding SImp data to real training samples yielded modest improvements in some cases. On the *iMove* dataset, where PriorMDM can accurately generate most activity classes, macro F1 increased from 0.636 to 0.739, representing a relative gain of 16.2%. However, performance on *iEat* declined from 0.718 to 0.651, likely due to a semantic mismatch between generated and real-world activities. On *ImpAct*, there is a loss of performance as well. These results highlight the potential but also the limitations of naively mixing synthetic and real data, underscoring the need for more structured integration strategies such as those used in SImpHARNet.

SImpHARNet Architecture Performance: SImpHARNet’s two-stage design—contrastive pretraining followed by task-specific fine tuning—enables robust representation learning from synthetic data and effective adaptation to real-world HAR. This architecture consistently outperforms both baseline and single-stage models across *ImpAct*, *iMove*, and *iEat*, particularly in low-data regimes. The encoder learns transferable features during pretraining, while the downstream classifier benefits from flexibility during fine-tuning, resulting in substantial gains in both macro F1 and accuracy.

Encoder Freezing vs. Late Learning: We compared two training regimes: (1) freezing the encoder, and (2) staged fine-tuning (Late Learning). The latter consistently yielded higher F1 scores (0.767 for *ImpAct*, 0.771 for *iMove*, 0.832 for *iEat*). Frozen models showed flatter performance curves across training data sizes, reflecting limited adaptability due to fixed encoder weights. In contrast, Late Learning leveraged additional data more effectively.

Embedding Dimension: We evaluated how bottleneck dimensionality affects performance given in Figure 6. Increasing embedding size from 16 to 256 improved F1 scores across all datasets, as larger vectors captured richer motion features. Gains plateaued beyond 256, with marginal improvement up to 1024. Peak F1 scores ranged from 0.753 to 0.832 at 256 or 512 dimensions. We chose 256 as a balance between accuracy and efficiency.

Training Data Size: To test data efficiency, we varied the training set size from 20% to 100% given in Figure 7. Across all datasets, Late Learning surpassed other strategies even with 60–80% of data. For instance, in *iEat*, it outperformed the full-data No Pretrain baseline

using only 60%. No Pretrain improved slowly with more data, while Frozen Pretrain was stable but less responsive, further validating the value of our staged pretraining approach.

5 Limitations

While our framework demonstrates strong performance across multiple datasets, it is subject to two significant limitations that highlight directions for future improvement. (1) *Limited Biophysical Fidelity:* The current framework does not explicitly model individual physiological factors such as tissue conductivity, hydration levels, or body composition, which can significantly influence real-world impedance signals. Additionally, the neural grounding model requires subject-specific impedance-pose data for calibration, limiting the framework’s ability to generalize across users without retraining. Integrating biophysical priors into the simulation process could enhance physiological realism. To reduce calibration overhead, few-shot learning, meta-learning, or conditioning on user metadata (e.g., height, weight, body type) may enable signal personalization without subject-specific ground-truth data. (2) *Evaluation Scope:* Our experiments are focused on upper-body activities using wrist-mounted electrodes and a relatively small, demographically narrow participant pool. As a result, generalizability to lower-body movements, alternative electrode placements, or more diverse populations remains untested. Expanding evaluations to include additional activity types, sensor locations (e.g., chest, thigh), and varied participant demographics can provide a broader assessment. Cross-dataset validation would further support claims of robustness.

6 Conclusion

We presented SImpHAR, the first simulation framework for generating realistic bio-impedance signals from 3D motion and text prompts, enabling scalable data synthesis for human activity recognition. Central to our pipeline is Pose2Imp, a physics-informed method that models impedance dynamics via shortest paths and soft-body deformation, and Text2Imp, which bridges language and motion using generative models. We introduced SImpHARNet, a two-stage training strategy that leverages contrastive pretraining on synthetic impedance-text pairs, followed by fine-tuning on limited real data. Extensive experiments on three Impedance based HAR datasets *ImpAct*, *iMove*, and *iEat*—demonstrated that SImpHARNet consistently outperforms state-of-the-art baselines, particularly in low-data regimes. Our ablations confirm the effectiveness of simulated impedance, contrastive objectives, and staged fine-tuning. Looking ahead, we aim to integrate physiological models into the simulation pipeline, support broader activity coverage and sensor placements, and explore domain adaptation techniques to enable zero-calibration deployment across users.

Acknowledgments

The research reported in this paper was supported by the BMBF in the project CrossAct (01IW21003) and IITP grant funded by the Korea government(MSIT) (No. RS-2019-II190079).

References

- [1] Sizhen Bian, Mengxi Liu, Bo Zhou, and Paul Lukowicz. 2022. The state-of-the-art sensing techniques in human activity recognition: A survey. *Sensors* 22, 12 (2022), 4596.
- [2] Sizhen Bian, Vitor F Rey, Peter Hevesi, and Paul Lukowicz. 2019. Passive capacitive based approach for full body gym workout recognition and counting. In *2019 IEEE International Conference on Pervasive Computing and Communications (PerCom)*. IEEE, 1–10.
- [3] Haofeng Chen, Gang Ma, Peng Wang, and Xiaojie Wang. 2021. A bio-impedance analysis method based on human hand anatomy for hand gesture recognition. *IEEE Transactions on Instrumentation and Measurement* 70 (2021), 1–10.
- [4] Jingyuan Cheng, Mathias Sundholm, Bo Zhou, Matthias Kreil, and Paul Lukowicz. 2014. Recognizing Subtle User Activities and Person Identity with Cheap Resistive Pressure Sensing Carpet. In *2014 International Conference on Intelligent Environments*. 148–153. doi:10.1109/IE.2014.29
- [5] Mathias Ciliberto, Vitor Fortes Rey, Alberto Calatroni, Paul Lukowicz, and Daniel Roggen. 2021. Opportunity++: A multimodal dataset for video-and wearable, object and ambient sensors-based human activity recognition. *Frontiers in Computer Science* 3 (2021), 792065.
- [6] L Minh Dang, Kyungbok Min, Hanxiang Wang, Md Jalil Piran, Cheol Hee Lee, and Hyeonjoon Moon. 2020. Sensor-based and vision-based human activity recognition: A comprehensive survey. *Pattern Recognition* 108 (2020), 107561.
- [7] Shohreh Deldari, Daniel V. Smith, Hao Xue, and Flora D. Salim. 2021. Time Series Change Point Detection with Self-Supervised Contrastive Predictive Coding. In *Proceedings of the Web Conference 2021 (WWW '21)*. ACM. doi:10.1145/3442381.3449903
- [8] Vitor Fortes Rey, Kamalveer Kaur Garewal, and Paul Lukowicz. 2021. Translating videos into synthetic training data for wearable sensor-based activity recognition systems using residual deep convolutional networks. *Applied Sciences* 11, 7 (2021), 3094.
- [9] Vitor Fortes Rey, Sungho Suh, and Paul Lukowicz. 2022. Learning from the best: contrastive representations learning across sensor locations for wearable activity recognition. In *Proceedings of the 2022 ACM International Symposium on Wearable Computers*. 28–32.
- [10] Rafael Gonzalez-Landaeta, Oscar Casas, and Ramon Pallas-Areny. 2008. Heart rate detection from plantar bioimpedance measurements. *IEEE transactions on Biomedical Engineering* 55, 3 (2008), 1163–1167.
- [11] Chuan Guo, Shihao Zou, Xinxin Zuo, Sen Wang, Wei Ji, Xingyu Li, and Li Cheng. 2022. Generating diverse and natural 3d human motions from text. In *Proceedings of the IEEE/CVF Conference on Computer Vision and Pattern Recognition*. 5152–5161.
- [12] Yujiao Hao, Xijian Lou, Boyu Wang, and Rong Zheng. 2022. Cromosim: A deep learning-based cross-modality inertial measurement simulator. *IEEE Transactions on Mobile Computing* (2022).
- [13] Mir Kanon Ara Jannat, Md Shafiqul Islam, Sung-Hyun Yang, and Hui Liu. 2023. Efficient Wi-Fi-based human activity recognition using adaptive antenna elimination. *IEEE Access* (2023).
- [14] Hyeokhyen Kwon, Catherine Tong, Harish Haresamudram, Yan Gao, Gregory D Abowd, Nicholas D Lane, and Thomas Ploetz. 2020. Imutube: Automatic extraction of virtual on-body accelerometry from video for human activity recognition. *Proceedings of the ACM on Interactive, Mobile, Wearable and Ubiquitous Technologies* 4, 3 (2020), 1–29.
- [15] Paula Lago, Moe Matsuki, Kohei Adachi, and Sozo Inoue. 2021. Using additional training sensors to improve single-sensor complex activity recognition. In *Proceedings of the 2021 ACM International Symposium on Wearable Computers (Virtual, USA) (ISWC '21)*. Association for Computing Machinery, New York, NY, USA, 18–22. doi:10.1145/3460421.3480421
- [16] Paula Lago, Tsuyoshi Okita, Shingo Takeda, and Sozo Inoue. 2018. Improving Sensor-based Activity Recognition Using Motion Capture as Additional Information. In *Proceedings of the 2018 ACM International Joint Conference and 2018 International Symposium on Pervasive and Ubiquitous Computing and Wearable Computers (Singapore, Singapore) (UbiComp '18)*. Association for Computing Machinery, New York, NY, USA, 118–121. doi:10.1145/3267305.3267596
- [17] Woojae Lee and SeongHwan Cho. 2015. Integrated all electrical pulse wave velocity and respiration sensors using bio-impedance. *IEEE Journal of Solid-State Circuits* 50, 3 (2015), 776–785.
- [18] Zikang Leng, Amitrajit Bhattacharjee, Hrudhai Rajasekhar, Lizhe Zhang, Elizabeth Bruda, Hyeokhyen Kwon, and Thomas Plötz. 2024. IMUGPT 2.0: Language-Based Cross Modality Transfer for Sensor-Based Human Activity Recognition. *arXiv preprint arXiv:2402.01049* (2024).
- [19] Jing Lin, Ailing Zeng, Haoqian Wang, Lei Zhang, and Yu Li. 2023. One-stage 3d whole-body mesh recovery with component aware transformer. In *Proceedings of the IEEE/CVF Conference on Computer Vision and Pattern Recognition*. 21159–21168.
- [20] Mengxi Liu, Hymalai Bello, Bo Zhou, Paul Lukowicz, and Jakob Karolus. 2024. iFace: Hand-Over-Face Gesture Recognition Leveraging Impedance Sensing. In *Proceedings of the Augmented Humans International Conference 2024*. 131–137.
- [21] Mengxi Liu, Vitor Fortes Rey, Yu Zhang, Lala Shakti Swarup Ray, Bo Zhou, and Paul Lukowicz. 2024. iMove: Exploring Bio-impedance Sensing for Fitness Activity Recognition. *arXiv preprint arXiv:2402.09445* (2024).
- [22] Mengxi Liu, Yu Zhang, Bo Zhou, Sizhen Bian, Agnes Grünerbl, and Paul Lukowicz. 2023. iEat: Human-food interaction with bio-impedance sensing. In *Adjunct Proceedings of the 2023 ACM International Joint Conference on Pervasive and Ubiquitous Computing & the 2023 ACM International Symposium on Wearable Computing*. 207–207.
- [23] Matthew Loper, Naureen Mahmood, Javier Romero, Gerard Pons-Moll, and Michael J Black. 2023. SMPL: A skinned multi-person linear model. In *Seminal Graphics Papers: Pushing the Boundaries, Volume 2*. 851–866.
- [24] James R Matthie. 2008. Bioimpedance measurements of human body composition: critical analysis and outlook. *Expert review of medical devices* 5, 2 (2008), 239–261.
- [25] Seungwhan Moon, Andrea Madotto, Zhaojiang Lin, Alireza Dirafzoon, Aparajita Saraf, Amy Bearman, and Babak Damavandi. 2022. Imu2clip: Multimodal contrastive learning for imu motion sensors from egocentric videos and text. *arXiv preprint arXiv:2210.14395* (2022).
- [26] Yazeed K Musallam, Nasser I AlFassam, Ghulam Muhammad, Syed Umar Amin, Mansour Alsulaiman, Wadood Abdul, Hamdi Altaheri, Mohamed A Bencherif, and Mohammed Algabri. 2021. Electroencephalography-based motor imagery classification using temporal convolutional network fusion. *Biomedical Signal Processing and Control* 69 (2021), 102826.
- [27] Duc-Anh Nguyen, Cuong Pham, and Nhien-An Le-Khac. 2023. Virtual Fusion with Contrastive Learning for Single Sensor-based Activity Recognition. *arXiv preprint arXiv:2312.02185* (2023).
- [28] Matthias Plappert, Christian Mandery, and Tamim Asfour. 2016. The kit motion-language dataset. *Big data* 4, 4 (2016), 236–252.
- [29] Alec Radford, Jong Wook Kim, Chris Hallacy, Aditya Ramesh, Gabriel Goh, Sandhini Agarwal, Girish Sastry, Amanda Askell, Pamela Mishkin, Jack Clark, et al. 2021. Learning transferable visual models from natural language supervision. In *International conference on machine learning*. PMLR, 8748–8763.
- [30] Lala Ray, Daniel Geißler, Bo Zhou, Paul Lukowicz, and Berit Greinke. 2024. Origami single-end capacitive sensing for continuous shape estimation of morphing structures. *Scientific Reports* 14, 1 (2024), 17448.
- [31] Lala Shakti Swarup Ray, Daniel Geißler, Mengxi Liu, Bo Zhou, Sungho Suh, and Paul Lukowicz. 2024. ALS-HAR: Harnessing Wearable Ambient Light Sensors to Enhance IMU-based HAR. *arXiv preprint arXiv:2408.09527* (2024).
- [32] Lala Shakti Swarup Ray, Daniel Geißler, Bo Zhou, Paul Lukowicz, and Berit Greinke. 2023. Capafoldable: self-tracking foldable smart textiles with capacitive sensing. *arXiv preprint arXiv:2307.05370* (2023).
- [33] Lala Shakti Swarup Ray, Vitor Fortes Rey, Bo Zhou, Sungho Suh, and Paul Lukowicz. 2023. PressureTransferNet: Human Attribute Guided Dynamic Ground Pressure Profile Transfer using 3D simulated Pressure Maps. *arXiv preprint arXiv:2308.00538* (2023).
- [34] Lala Shakti Swarup Ray, Bo Zhou, Sungho Suh, Lars Krupp, Vitor Fortes Rey, and Paul Lukowicz. 2024. Text me the data: Generating Ground Pressure Sequence from Textual Descriptions for HAR. In *2024 IEEE International Conference on Pervasive Computing and Communications Workshops and other Affiliated Events (PerCom Workshops)*. 461–464. doi:10.1109/PerComWorkshops59983.2024.10503379
- [35] Lala Shakti Swarup Ray, Bo Zhou, Sungho Suh, and Paul Lukowicz. 2023. Pressim: An end-to-end framework for dynamic ground pressure profile generation from monocular videos using physics-based 3d simulation. In *2023 IEEE International Conference on Pervasive Computing and Communications Workshops and other Affiliated Events (PerCom Workshops)*. IEEE, 484–489.
- [36] Vitor Fortes Rey, Lala Shakti Swarup Ray, Xia Qingxin, Kaishun Wu, and Paul Lukowicz. 2024. Enhancing Inertial Hand based HAR through Joint Representation of Language, Pose and Synthetic IMUs. *arXiv preprint arXiv:2406.01316* (2024).
- [37] Matthias Ring, Clemens Lohmueller, Manfred Rauh, Joachim Mester, and Björn M Eskofier. 2015. A temperature-based bioimpedance correction for water loss estimation during sports. *IEEE journal of biomedical and health informatics* 20, 6 (2015), 1477–1484.
- [38] Kaan Sel, Deen Osman, and Roozbeh Jafari. 2021. Non-invasive cardiac and respiratory activity assessment from various human body locations using bioimpedance. *IEEE open journal of engineering in medicine and biology* 2 (2021), 210–217.
- [39] Yonatan Shafir, Guy Tevet, Roy Kapon, and Amit H Bermanno. 2023. Human motion diffusion as a generative prior. *arXiv preprint arXiv:2303.01418* (2023).
- [40] David Strömback, Sangxia Huang, and Valentin Radu. 2020. Mm-fit: Multimodal deep learning for automatic exercise logging across sensing devices. *Proceedings of the ACM on Interactive, Mobile, Wearable and Ubiquitous Technologies* 4, 4 (2020), 1–22.
- [41] Hongjin Su, Weijia Shi, Jungo Kasai, Yizhong Wang, Yushi Hu, Mari Ostendorf, Wen-tau Yih, Noah A Smith, Luke Zettlemoyer, and Tao Yu. 2022. One embedder, any task: Instruction-finetuned text embeddings. *arXiv preprint arXiv:2212.09741* (2022).
- [42] Sungho Suh, Vitor Fortes Rey, Sizhen Bian, Yu-Chi Huang, Jože M Rožanec, Hooman Tavakoli Ghinani, Bo Zhou, and Paul Lukowicz. 2023. Worker Activity

- Recognition in Manufacturing Line Using Near-body Electric Field. *IEEE Internet of Things Journal* (2023).
- [43] Chi Ian Tang, Ignacio Perez-Pozuelo, Dimitris Spathis, and Cecilia Mascolo. 2020. Exploring contrastive learning in human activity recognition for healthcare. *arXiv preprint arXiv:2011.11542* (2020).
- [44] Laurens Van der Maaten and Geoffrey Hinton. 2008. Visualizing data using t-SNE. *Journal of machine learning research* 9, 11 (2008).
- [45] Huiyuan Yang, Han Yu, Kusha Sridhar, Thomas Vaessen, Inez Myin-Germeys, and Akane Sano. 2022. More to Less (M2L): Enhanced health recognition in the wild with reduced modality of wearable sensors. In *2022 44th Annual International Conference of the IEEE Engineering in Medicine & Biology Society (EMBC)*. IEEE, 3253–3256.
- [46] Naoya Yoshimura, Jaime Morales, Takuya Maekawa, and Takahiro Hara. 2024. Openpack: A large-scale dataset for recognizing packaging works in iot-enabled logistic environments. In *2024 IEEE International Conference on Pervasive Computing and Communications (PerCom)*. IEEE, 90–97.
- [47] Alexander D Young, Martin J Ling, and Damal K Arvind. 2011. IMUSim: A simulation environment for inertial sensing algorithm design and evaluation. In *Proceedings of the 10th ACM/IEEE International Conference on Information Processing in Sensor Networks*. IEEE, 199–210.
- [48] Bo Zhou, Mathias Sundholm, Jingyuan Cheng, Heber Cruz, and Paul Lukowicz. 2016. Never skip leg day: A novel wearable approach to monitoring gym leg exercises. In *2016 IEEE International Conference on Pervasive Computing and Communications (PerCom)*. IEEE, 1–9.
- [49] Yexu Zhou, Haibin Zhao, Yiran Huang, Till Riedel, Michael Hefenbrock, and Michael Beigl. 2022. Tinyhar: A lightweight deep learning model designed for human activity recognition. In *Proceedings of the 2022 ACM International Symposium on Wearable Computers*. 89–93.
- [50] Henrik Zimmer, Marcel Campen, and Leif Kobbelt. 2013. Efficient computation of shortest path-concavity for 3D meshes. In *Proceedings of the IEEE Conference on Computer Vision and Pattern Recognition*. 2155–2162.
- [51] Parham Zolfaghari, Vitor Fortes Rey, Lala Ray, Hyun Kim, Sungho Suh, and Paul Lukowicz. 2024. Sensor Data Augmentation from Skeleton Pose Sequences for Improving Human Activity Recognition. In *2024 International Conference on Activity and Behavior Computing (ABC)*. IEEE, 1–8.